The Journal of Neuroscience, November 15, 2002, 22(22):9776–9784

Rab11a and Myosin Vb Regulate Recycling of the M_4 Muscarinic Acetylcholine Receptor

Laura A. Volpicelli,[1] James J. Lah,[1] Guofu Fang,[1] James R. Goldenring,[2] and Allan I. Levey[1]

[1]*Center for Neurodegenerative Disease and Department of Neurology, Emory University School of Medicine, Atlanta, Georgia 30322, and* [2]*Department of Surgery, Vanderbilt University School of Medicine, Nashville, Tennessee 37232*

Agonist-induced internalization followed by subsequent return to the cell surface regulates G-protein-coupled receptor (GPCR) activity. Because the cellular responsiveness to ligand depends on the balance between receptor degradation and recycling, it is crucial to identify the molecules involved in GPCR recovery to the cell surface. In this study, we identify mechanisms involved in the recycling of the M_4 subtype of muscarinic acetylcholine receptor. M_4 is highly expressed in the CNS, plays a role in locomotor activity, and is a novel therapeutic target for neurologic and psychiatric disorders. Previous studies show that, after cholinergic stimulation, M_4 internalizes from the cell surface to endosomes in cell culture and the rat brain. Here, we show that, after activation, M_4 traffics to transferrin receptor- and Rab11a-positive perinuclear endosomes. Expression of the constitutively GDP-bound, inactive mutant Rab11aS25N inhibits M_4 trafficking to recycling endosomes. Expression of the C-terminal tail of myosin Vb, a Rab11a effector, enhances M_4 accumulation in perinuclear endosomes. Both Rab11aS25N and the myosin Vb tail impair M_4 recycling. The results demonstrate that GPCR recycling is mediated through a discrete pathway using both Rab11a and myosin Vb.

Key words: PC12 cells; muscarinic acetylcholine receptors; G-protein-coupled receptor; M_4; recycling; endosomes; Rab11a; myosin Vb; unconventional myosins; transferrin receptor; endocytosis; internalization

Regulated intracellular trafficking after stimulation controls activity and cell surface expression of neurotransmitter receptors, including G-protein-coupled receptors (GPCRs) and ion channels (Koenig and Edwardson, 1997; Lefkowitz, 1998; Carroll et al., 2001; Roche et al., 2001; St. John and Gordon, 2001). Agonist-induced GPCR internalization has been demonstrated in cell culture and in the rat and human brain (Bloch et al., 1999; Muriel et al., 1999). The balance between GPCR internalization and recycling to the cell surface or degradation dictates the neuronal responsiveness to ligand. Furthermore, GPCR trafficking plays a role in the physiological tolerance to drugs (Whistler et al., 1999; Finn and Whistler, 2001; He et al., 2002). Because most treatments of CNS disorders include long-term administration of agonists that target GPCRs, drug development and therapeutics depend on gaining a better understanding of the intracellular fate of GPCRs.

Early endosomes comprise distinct compartments identified primarily through studies of trafficking of the transferrin receptor (TfnR), a single transmembrane receptor that constitutively internalizes. At steady state, the TfnR resides in perinuclear recycling endosomes that are distinguished from other endosomes by selective retention of recycling proteins and the presence of the small GTPase Rab11a (Hopkins et al., 1994; Ullrich et al., 1996; Green et al., 1997). Rab11a (Ullrich et al., 1996; Ren et al., 1998) and myosin Vb, a member of the class V unconventional myosins (Lapierre et al., 2001) that interacts with Rab11a, are involved in TfnR recycling to the plasma membrane.

Although mechanisms involved in agonist-induced GPCR endocytosis have been extensively characterized, less is known about the intracellular pathways and molecules involved in GPCR recycling. The mechanisms mediating GPCR recycling may be distinct from those for the constitutively recycling TfnR (Cao et al., 1999). Also, different GPCR subtypes show distinct endocytic trafficking patterns (Trejo and Coughlin, 1999; Anburgh et al., 2000; Krudewig et al., 2000; Tsao and von Zastrow, 2000; Innamorati et al., 2001). Given the central role that GPCR recycling plays in regulating cellular responses to ligand, it is critical to identify the mechanisms that control GPCR recycling. Furthermore, because the mechanisms that control TfnR trafficking do not necessarily generalize to GPCRs and because the different GPCR subtypes show distinct endocytic pathways, it is crucial to characterize the intracellular trafficking of individual GPCR subtypes.

We examined the pathways responsible for the recycling of the M_4 muscarinic ACh receptor (mAChR). M_4 is highly expressed in the CNS (Levey et al., 1991; Hersch et al., 1994), is the primary autoreceptor in the striatum, plays a role in locomotor activity (Gomeza et al., 1999), and is a novel therapeutic target for schizophrenia (Felder et al., 2001) and Alzheimer's disease (Bodick et al., 1997). Activated M_4 internalizes to endosomes in cell culture and the rat brain, and M_4 recycling to the plasma membrane is required for resensitization (Bogatkewitsch et al., 1996; Bernard et al., 1999; Volpicelli et al., 2001). To define the mechanisms that control receptor recycling, we studied the endogenously expressed M_4 mAChR in neuronotypic PC12 cells (Berkeley and Levey, 2000). This study identifies Rab11a and

Received July 17, 2002; revised Sept. 9, 2002; accepted Sept. 11, 2002.

This work was supported by the Alzheimer's Association (A.I.L.), a Pharmaceutical Research and Manufacturers Association Foundation Advanced Predoctoral Fellowship (L.A.V.), National Institutes of Health Grant RO1 NS30454 (A.I.L.), National Institutes of Health/National Institute of Diabetes and Digestive and Kidney Diseases Grants DK48370 and DK43405, and a Veterans Administration Merit Award (J.R.G.).

Correspondence should be addressed to Dr. A. I. Levey, Center for Neurodegenerative Disease, Emory University School of Medicine, Whitehead Biomedical Research Building, 615 Michael Street, Fifth Floor, Atlanta, GA 30322. E-mail: alevey@emory.edu.

myosin Vb as critical regulators of GPCR return to the plasma membrane.

MATERIALS AND METHODS

cDNA constructs. The Rab11aS25N construct was a generous gift from Dr. Marino Zerial (Max Planck Institute for Molecular Cell Biology and Genetics, Dresden, Germany) (Ullrich et al., 1996). To construct the GFP-Rab11aS25N plasmid, the Rab11aS25N cDNA was amplified by PCR with a 5′ primer (5′-TTATATCTCGAGAATGGGCACCCGCGA-3′) that introduced a *Xho*I restriction enzyme site and a 3′ primer (5′-CGCGCGGAATTCGCCTTATATGTTCTG-3′) that introduced an *Eco*RI restriction enzyme site. The products were digested and ligated into the pEGFP-C2 (Clontech, Palo Alto, CA) vector. The sequence of the Rab11aS25N construct was confirmed by MWG Biotech (High Point, NC). The myosin Vb tail–GFP construct has been described previously (Lapierre et al., 2001).

Cell culture and transfections. PC12 cells were maintained at 37°C and 5% CO_2 in DMEM (Mediatech, Herndon, VA) containing 10% heat-inactivated horse serum (Invitrogen, Grand Island, NY), 5% fetal clone serum (HyClone, Logan, UT), and 1% penicillin–streptomycin. Cells grown in six-well trays were transfected with 1 μg of plasmid DNA using LipofectAMINE 2000 (Invitrogen, Carlsbad, CA). Approximately 5 hr after the transfection, the cells were rinsed three times with PBS and passaged onto Matrigel-coated coverslips in six-well trays. Immunocytochemistry was performed 2 d after transfections.

Analysis of M_4 recycling. To selectively examine the proportion of internalized receptors that return to the cell surface, newly synthesized receptors were eliminated by 30 min pretreatment with cycloheximide (20 μg/ml) (Szekeres et al., 1998). Cycloheximide was also included in all subsequent drug treatments. Cells were treated with media containing 100 μM carbachol (CCh) for 60 min to induce M_4 internalization. The dishes were then placed on ice, rinsed two times with chilled DMEM, returned to 37°C, and incubated with media containing cycloheximide for various time points. To calculate M_4 recycling, the percentage of M_4 colocalization with cell surface Na^+/K^+ ATPase after CCh washout was quantified (see below) and normalized to cell surface M_4 in untreated cells. The residual cell surface M_4 remaining after 60 min CCh treatment was then subtracted from this value to obtain the amount of M_4 that recovers to the cell surface after CCh treatment and washout.

Immunocytochemistry. Cells were fixed for 30 min with 2% paraformaldehyde in 0.1 M phosphate buffer, pH 7.3 and rinsed several times with PBS containing 0.5 normal horse serum (PBS^+). The cells were blocked with PBS containing 5% normal horse serum and 1% bovine serum albumin (blocking buffer) and permeabilized with 0.05% Triton X-100. The cells were rinsed several times with PBS^+ and incubated in primary antibody diluted in blocking buffer overnight at 4°C. For double labeling, both primaries were included in the incubation. The following primary antibodies were used: early endosome autoantigen 1 (EEA1) mouse monoclonal (1:250; Transduction Laboratories, Lexington KY); M_4 mouse monoclonal (1:500; Chemicon, Temecula, CA) (Bernard et al., 1999) or rabbit polyclonal (0.5 μg/ml) (Levey et al., 1991); Na^+/K^+ ATPase α-1 subunit mouse monoclonal (1:500; Upstate Biotechnology, Lake Placid, NY); Rab4 rabbit polyclonal (1:500; Biosource, Camarillo, CA), Rab7 rabbit polyclonal (1:100) (Chavrier et al., 1990), or Rab11 rabbit polyclonal (1:500; Zymed, San Francisco, CA); and TfnR mouse monoclonal (1:500; Zymed). The cells were rinsed and incubated for 60 min with rhodamine red-X or Cy5-conjugated donkey anti-rabbit or mouse secondary antibodies diluted in blocking buffer (1:100; Jackson ImmunoResearch, West Grove, PA). Both secondary antibodies were included in the incubation. The cells were then rinsed and mounted onto slides with Vectashield mounting medium (Vector Laboratories, Burlingame, CA). The cells were scanned with a Zeiss (Heidelberg, Germany) LSM 510 laser scanning confocal microscope as described previously (Volpicelli et al., 2001), and the images were prepared using Adobe Photoshop (Adobe Systems, San Jose, CA).

Quantitation of colocalization. MetaMorph imaging system software (Universal Imaging Corporation, West Chester, PA) was used to quantitate colocalization on unprocessed images as described previously (Volpicelli et al., 2001). Briefly, background was subtracted from the images, and the percentage of overlapping pixels between M_4 and Na^+/K^+ ATPase (or other markers) pixels was determined. Unless indicated otherwise, for each time point, eight cells from three experiments were analyzed for $n = 24$. All data were analyzed by independent samples *t* test or ANOVA and Fisher's least significant difference *post hoc* test.

Binding assays. After drug treatments, cells plated on six-well trays were rinsed three times with 2 ml of cold HBSS (Mediatech) and incubated overnight at 4°C with 1 nM ^{3}H-quinuclidinyl benzilate (QNB) or 1 nM ^{3}H-*N*-methyl-scopolamine (NMS). Nonspecific binding was determined using 20 μM atropine. The cells were transferred to polystyrene culture tubes and filtrated through Whatman GF/B fired glass-fiber filters. Filters were rinsed three times with cold PBS, and radioactivity was determined by liquid scintillation spectroscopy.

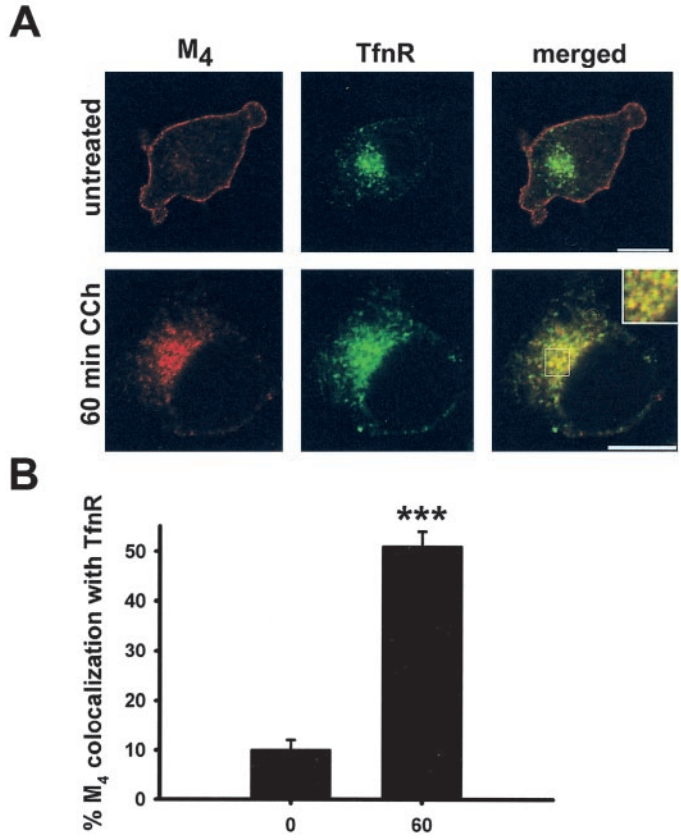

Figure 1. After agonist stimulation, M_4 traffics to a perinuclear compartment, in which it colocalizes with the TfnR. *A*, In untreated PC12 cells, M_4 (*red*) localized to the cell surface, and the TfnR (*green*) showed a primarily perinuclear distribution. After 60 min continuous CCh treatment, M_4 redistributed from the cell surface to the perinuclear compartment, in which it colocalized extensively with the TfnR (visualized as *yellow* in the merged images). The *inset* shows a higher-magnification image of the perinuclear compartment, demonstrating that the majority of internalized M_4 colocalized with the TfnR. Scale bar, 10 μm. *B*, Quantitation of confocal images demonstrated that M_4 showed minimal colocalization with TfnR in untreated cells ($n = 11$), and, after 60 min CCh treatment, M_4 overlap with TfnR was significantly enhanced ($n = 16$). $^{***}p < 0.001$.

RESULTS

After prolonged agonist stimulation, M_4 traffics to a TfnR-positive perinuclear compartment

In nonpolarized cells, the constitutively endocytosed and recycled TfnR localizes to a perinuclear compartment defined as recycling endosomes (Hopkins et al., 1994). To begin to study the role of this endosomal compartment in M_4 recycling, we determined whether M_4 colocalizes with the TfnR after sustained agonist stimulation (Fig. 1*A*). In untreated PC12 cells, M_4 localized primarily to the cell surface, whereas the TfnR showed a concentrated localization near the nucleus. Brief stimulation with CCh (10 min) resulted in M_4 internalization to peripherally distributed early endosomes (Volpicelli et al., 2001). After pro-

longed (60 min) CCh stimulation, M_4 internalized from the cell surface and showed a perinuclear localization similar to the TfnR. M_4 and the TfnR colocalized extensively in this perinuclear endosomal compartment, indicating that M_4 traveled to a similar recycling endosomal compartment as the TfnR after agonist stimulation. Quantitation of the confocal images revealed minimal colocalization of M_4 with the TfnR in untreated cells and a significant increase of M_4 overlap with TfnR after 60 min prolonged CCh treatment.

After agonist washout, M_4 returns to the cell surface

After prolonged CCh treatment, M_4 may either recycle to the cell surface or be targeted to lysosomes for degradation. We therefore determined whether internalized M_4 returns to the cell surface after agonist washout. To distinguish receptors that recycle to the cell surface after agonist treatment and internalization from newly synthesized receptors, cells were pretreated with cycloheximide to prevent new protein synthesis. In nonstimulated cells, M_4 showed colocalization with the cell surface marker Na^+/K^+ ATPase (Fig. 2*A*). After CCh treatment, internalized M_4 resided near the nucleus and showed minimal overlap with the Na^+/K^+ ATPase. However, by 60 min of CCh washout, M_4 returned to the cell surface, in which it colocalized with the Na^+/K^+ ATPase. A portion of M_4 remained in an intracellular localization 60 min after CCh washout.

To quantitate recycling after agonist washout, M_4 overlap with the cell surface marker Na^+/K^+ ATPase was measured on confocal images. Using this method to quantify M_4 internalization in single cells has been established previously and shown to provide results similar to measurements of internalization use binding assays with the membrane impermeant, nonselective mAChR ligand ^{3}H-NMS (Volpicelli et al., 2001). We first compared the extent of M_4 recycling measured by quantitative immunocytochemistry with binding assays using ^{3}H-NMS (Fig. 2*B*). Cells were treated with CCh for 60 min, rinsed, and incubated in media alone for 60 or 90 min. When the recycling data obtained from confocal images and binding assays were expressed as a percentage of untreated cells, the extent of M_4 recycling measured by quantitative immunocytochemistry was slightly higher than binding assay measurements. It is possible that measuring the percentage of M_4 pixels that overlap with the Na^+/K^+ ATPase after CCh treatment and washout included receptors that are at or near the cell surface but cannot bind ligand. When the cell surface M_4 remaining after 60 min CCh treatment was subtracted from the value of cell surface M_4 after CCh washout, the values for M_4 recycling were equivalent to binding assays. Therefore, quantitative immunocytochemistry provides a valid measure of M_4 recycling after agonist stimulation and washout, and this method of calculating M_4 recycling was used for all of the analysis throughout the paper. Furthermore, unlike binding assays, confocal microscopy allows visualization of M_4 localization to specific intracellular compartments.

Quantitative immunocytochemistry was then used to analyze a more extensive time course of M_4 recycling (Fig. 2*C*). M_4 began to recycle to the plasma membrane as early as 15 min after CCh washout, and, by 3 hr, the vast majority of detectable M_4 had returned to the cell surface ($t_{1/2}$ = 60 min).

It is possible that two sources of intracellular of M_4 could contribute to the reappearance of M_4 to the cell surface: M_4 internalized after agonist stimulation and a pool of intracellular M_4 that existed at baseline. We therefore measured the numbers of cell surface mAChRs (using the membrane-impermeant ligand

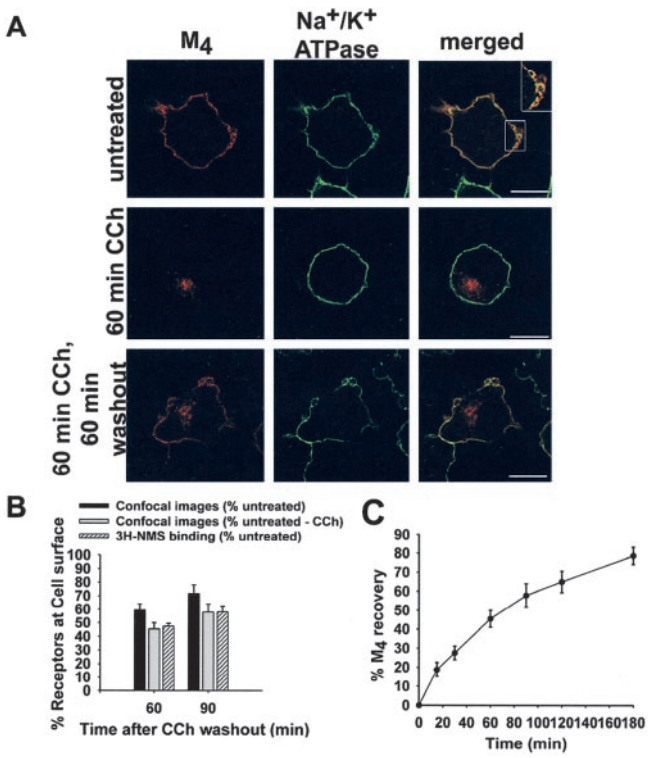

Figure 2. M_4 returns to the cell surface after agonist stimulation and washout. To selectively examine the amount of M_4 that recycles to the cell surface after CCh treatment and washout, cells were treated with cycloheximide to prevent new receptor synthesis, and cycloheximide was included in all subsequent drug treatments. *A*, Cells were untreated, treated continuously with CCh for 60 min, or treated with CCh for 60 min, rinsed, and incubated in media alone for 60 min to allow M_4 recovery to the cell surface. In untreated cells, M_4 (*red*) localized primarily to the cell surface, but a small proportion of receptors also showed an intracellular localization. Cell surface M_4 colocalized (*yellow* in the merged image) with the plasma membrane marker Na^+/K^+ ATPase (*green*). The *inset* shows a higher-magnification image of the cell surface, demonstrating that, although M_4 showed colocalization with the Na^+/K^+ ATPase (*yellow*), subdomains exist at the cell surface that contain M_4 but not the Na^+/K^+ ATPase (*red*). Although all cells show staining for the Na^+/K^+ ATPase, not all PC12 cells show M_4 staining, demonstrating heterogeneity of M_4 receptor expression in PC12 cells. After 60 min continual CCh treatment, M_4 trafficked from the cell surface to perinuclear endosomes and no longer colocalized with Na^+/K^+ ATPase. After 60 min CCh treatment followed by 60 min washout, M_4 returned to the cell surface, in which it colocalized with the Na^+/K^+ ATPase. A proportion of receptors also showed an intracellular distribution. Scale bars, 10 μm. *B*, Measurements of M_4 recycling using quantitative immunocytochemistry were compared with measurements of mAChR recycling using ^{3}H-NMS. Cells were treated with CCh, rinsed, and incubated in media alone for 60 or 90 min. The amounts of cell surface receptors measured using both assays after CCh washout were normalized to the amounts of cell surface receptors in untreated cells (*black bars* and *cross-hatched bars*). When expressed as a percentage of untreated cells, the extent of M_4 recycling measured by quantitative immunocytochemistry was slightly higher than the extent of recycling measured by binding assays. Subtracting the residual M_4 remaining after 60 min CCh treatment, however, produced values for M_4 recycling using confocal images (*gray bars*) that were similar to measurements of mAChR recycling using binding assays. This method of calculating M_4 recycling in confocal images was thus used throughout the remainder of the paper. *C*, The amount of M_4 recovery to the cell was quantified using confocal images at various time points after CCh washout. The graph demonstrates that M_4 began to return to the cell surface as early as 15 min after agonist washout, and, 3 hr after washout, the majority of M_4 (visible by immunocytochemistry) localized to the cell surface.

^{3}H-NMS) and total mAChRs (using the permeable ligand ^{3}H-QNB). The vast majority (96%) of mAChRs reside at the cell surface in untreated PC12 cells. Unlike binding assays, confocal images show a proportion of intracellular M_4 in unstimulated cells (Fig. 2), and measurements of pixel intensity reveal that ~20% of M_4 pixels represent an intracellular pool of receptors. Intracellular M_4 could reside in acidic endosomes or lysosomes in which the receptor conformation is altered, or the receptor is degraded such that it cannot be recognized by ligand but can be recognized by the antibody. Prolonged treatment of control PC12 cells with atropine to prevent M_4 activation and internalization by endogenously released ACh does not cause a statistically significantly increase of M_4 colocalization with the Na^+/K^+ ATPase (Volpicelli et al., 2001). Thus, the intracellular M_4 detected by immunofluorescence in unstimulated cells does not traffic to the cell surface and therefore does not substantially contribute to the reappearance of M_4 at the cell surface.

Although quantitative immunocytochemistry can analyze receptor distribution within a cell (i.e., the percentage of detectable receptor at the cell surface vs intracellular), it does not provide information about possible changes in total receptor levels. Therefore, binding assays using ^{3}H-QNB, which binds to cell surface and intracellular mAChRs, were performed to measure the extent of mAChR degradation after CCh stimulation and washout. After 60 min CCh treatment, total mAChR binding was unchanged (110 ± 15% of untreated cells). Because M_4 accounts for >95% of total mAChR binding in PC12 cells (Berkeley and Levey, 2000), the majority of M_4 does not degrade after 60 min continual CCh treatment. However, after 60 min CCh treatment followed by 180 min washout, mAChR binding was 57 ± 4% of untreated cells. Therefore, after prolonged CCh treatment, ~40% of M_4 was targeted for degradation and the remaining M_4 returned to the cell surface.

Internalized M_4 traffics to a Rab11a-positive perinuclear compartment

In nonpolarized cells, Rab11a shows a perinuclear distribution similar to internalized M_4 and TfnR and plays a role in TfnR recycling back to the cell surface in HeLa, CHO, and BHK cells (Ullrich et al., 1996; Ren et al., 1998). We determined whether M_4 also colocalized with Rab11a in the TfnR-positive compartment of CCh-treated PC12 cells. Initially after CCh stimulation (2.5 and 10 min), M_4 began to internalize from the cell surface, and the majority of M_4 localized to discrete puncta distributed peripherally throughout the cell (Fig. 3*A*), shown previously to be EEA1-positive endosomes (Volpicelli et al., 2001). Although the majority of M_4 did not colocalize with Rab11a after 2.5 min of CCh stimulation, by 10 min CCh, a significant portion of M_4 accumulated near the nucleus, in which it colocalized with Rab11a. After 60 min continual CCh treatment, the majority of M_4 colocalized with Rab11a in the perinuclear compartment. Quantitation of M_4 colocalization with Rab11a (Fig. 3*B*) showed that the extent of M_4 colocalization with Rab11a progressively increased over the time course of CCh treatment.

Perinuclear concentration of internalized M_4 is Rab11a dependent

To determine whether M_4 trafficking to perinuclear endosomes required Rab11a GTPase activity, we expressed, in PC12 cells, the constitutively GDP-bound GFP-Rab11aS25N fusion protein, which cannot exchange GDP for GTP. GFP-Rab11aS25N showed a diffuse, cytosolic distribution consistent with the inability of

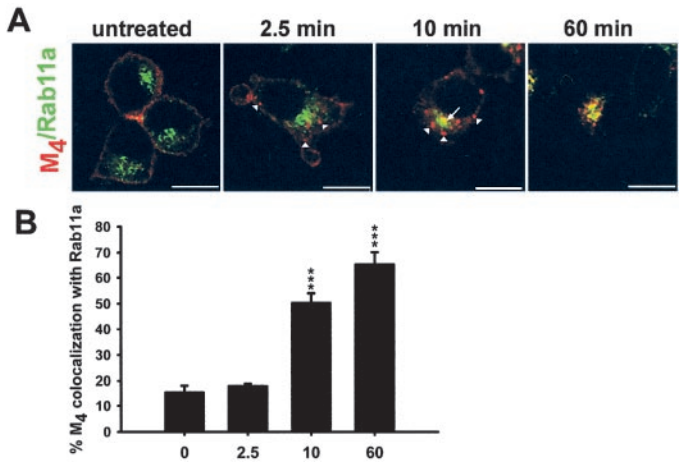

Figure 3. After prolonged CCh stimulation, M_4 colocalizes with Rab11a in the perinuclear compartment. *A*, After 2.5 min continual CCh treatment, M_4 (*red*) began to redistribute from the cell surface to large puncta (*arrowheads*) that did not colocalize with Rab11a (*green*). M_4 began to colocalize with Rab11a after 10 min CCh treatment (visualized as *yellow*, *arrow*), and, after 60 min, M_4 colocalized extensively with Rab11a in the perinuclear compartment. Scale bars, 10 μm. *B*, Quantitation of confocal images demonstrated that M_4 showed minimal colocalization with Rab11a in untreated cells ($n = 7$) and after 2.5 min CCh stimulation ($n = 4$). By 10 min of continual CCh treatment ($n = 9$), M_4 overlap with Rab11a was significantly enhanced and increased further after 60 min CCh treatment ($n = 12$). $^{***}p < 0.001$.

GDP-bound Rab proteins to bind to the membrane (Ullrich et al., 1994) (Fig. 4*A*). In untreated PC12 cells, expression of GFP-Rab11aS25N had no effect on the localization of M_4 to the plasma membrane (data not shown). In control cells transfected with the pEGFP vector, after 60 min CCh, internalized M_4 showed a perinuclear localization. In cells expressing GFP-Rab11aS25N, M_4 localized to small puncta dispersed throughout the cell and did not concentrate near the nucleus. Similarly, expression of GFP-Rab11aS25N also dispersed the TfnR throughout the cell compared with pEGFP vector-transfected control cells (Fig. 4*B*). M_4 showed colocalization with TfnR in vector-transfected control cells and in Rab11aS25N-expressing cells. Quantitative immunocytochemistry revealed that M_4 colocalization with the TfnR in vector-transfected cells (51 ± 3%; $n = 16$) was equivalent to GFP-Rab11aS25N-transfected cells (50 ± 4%; $n = 16$; p = NS).

It has been proposed that constitutively GDP-bound Rab11aS25N prevents trafficking of the TfnR from early endosomes to perinuclear recycling endosomes (Ullrich et al., 1996; Ren et al., 1998). Because GFP-Rab11aS5N impairs M_4 trafficking to perinuclear endosomes, we sought to identify the peripheral vesicular compartment containing M_4 in cells expressing this mutant. First, we analyzed the extent of M_4 colocalization with the early endosome marker EEA1 (Rubino et al., 2000). In both pEGFP-transfected and GFP-Rab11aS25N-expressing cells, EEA1 localized to large puncta throughout the cell (Fig. 5*A*). However, in both cases, after 60 min CCh treatment, we failed to observe significant overlap between EEA1 and M_4. Quantitative immunocytochemistry showed that M_4 colocalization with EEA1 in Rab11aS25N-expressing cells (19 ± 3%; $n = 16$) was not increased compared with vector-transfected control cells (22 ± 6%; $n = 16$; p = NS). If GFP-Rab11a S25N prevented trafficking from EEA1-positive early endosomes, M_4 colocalization with EEA1 would be enhanced relative to control cells. However, although M_4 shows a more dispersed localization in Rab11aS25N-

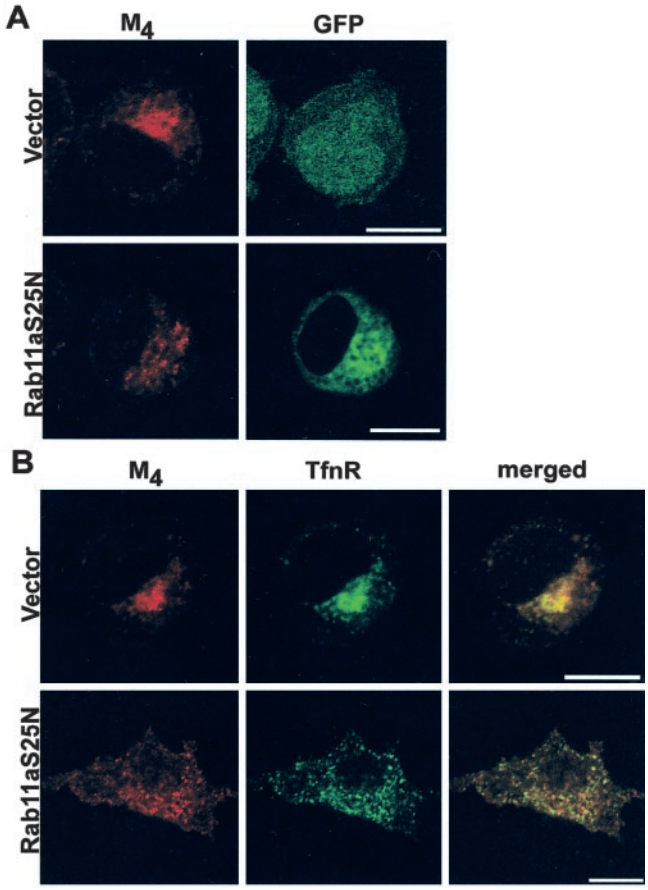

Figure 4. Constitutively GDP-bound Rab11aS25N prevents M_4 accumulation in perinuclear recycling endosomes. Cells were treated continuously with CCh for 60 min. *A*, In control cells transfected with the pEGFP vector, GFP showed a diffuse, ubiquitous distribution, and M_4 (*red*) localized to the perinuclear compartment. In cells transfected with GFP-Rab11aS25N, GFP showed a diffuse, cytosolic distribution consistent with the inability of GDP-bound Rab11aS25N to bind membrane. In contrast to vector-transfected control cells, M_4 in cells expressing GFP-Rab11aS25N localized to small puncta distributed throughout the cell and did not accumulate in the perinuclear compartment. Scale bars, 10 μm. *B*, In pEGFP vector-transfected control cells, M_4 (*red*) and TfnR (*green*) localized to the perinuclear compartment. Expression of GFP-Rab11aS25N caused dispersal of both M_4 and TfnR to small puncta distributed throughout the cell. M_4 and TfnR showed colocalization in both vector-transfected control cells and GFP-Rab11aS25N-expressing cells. Scale bars, 10 μm.

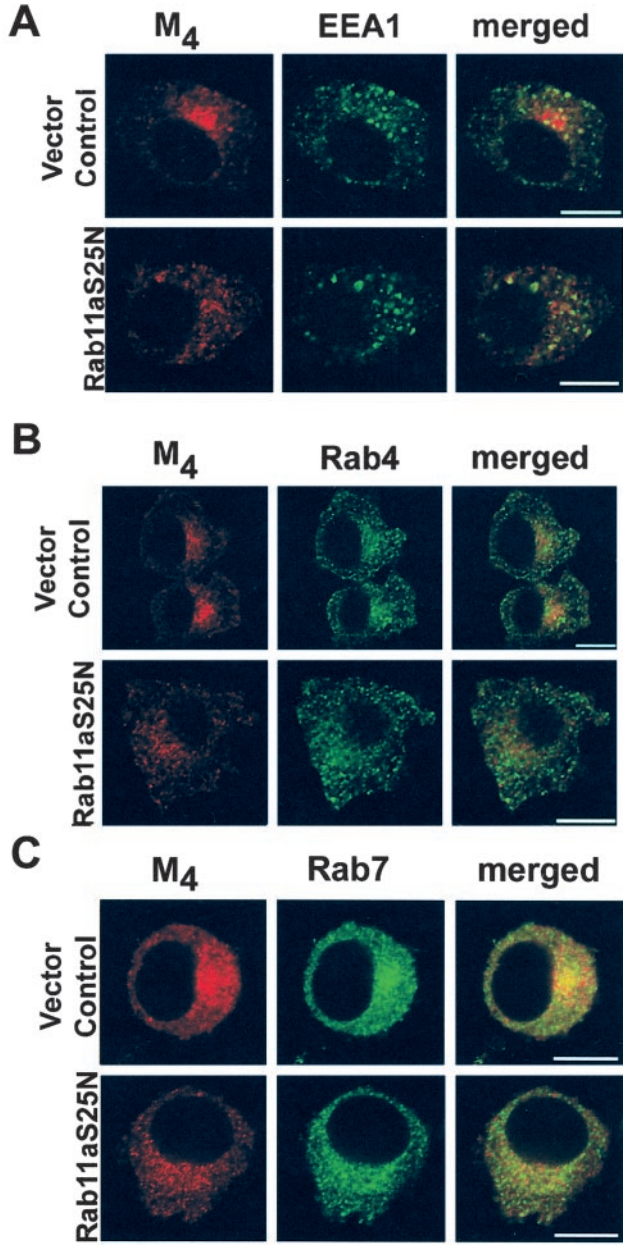

Figure 5. Constitutively GDP-bound Rab11aS25N does not prevent M_4 transit through early endosomes or enhance M_4 trafficking to late endosomes. Cells were treated continuously with CCh for 60 min. *A*, In vector-transfected control cells, the early endosomal marker EEA1 (*green*) localized to puncta distributed peripherally throughout the cell, and M_4 and EEA1 showed minimal colocalization. In cells transfected with GFP-Rab11aS25N, M_4 localized to small puncta dispersed throughout the cell. However, M_4 and EEA1 showed little colocalization. Scale bars, 10 μm. *B*, Rab4 (*green*) localized to small puncta peripherally distributed throughout the cell. M_4 (*red*) showed minimal colocalization with Rab4 in vector-transfected control cells and cells expressing Rab11aS25N. Scale bars, 10 μm. *C*, The late endosomal marker Rab7 localized to small puncta distributed throughout the cells. In vector-transfected control cells, internalized M_4 showed some colocalization with Rab7. In cells expressing GFP-Rab11aS25N, M_4 colocalization with Rab7 was not enhanced. Scale bars, 10 μm.

expressing cells compared with vector-transfected control cells, M_4 colocalization with EEA1 is not enhanced. Therefore, M_4 can exit from the EEA1-positive early endosomal domain in cell expressing dominant negative Rab11aS25N.

Early endosomes are comprised of two domains: a Rab5a/EEA1 domain that initially receives endocytosed material and a Rab4 domain. Rab4 is involved in recycling of the TfnR and the β-adrenergic receptor directly from early endosomes (van der Sluijs et al., 1992; Seachrist et al., 2000; Sonnichsen et al., 2000). It was thus possible that, in the presence of GFP-Rab11aS25N, M_4 could transit from the EEA1-positive early endosomal domain to the Rab4-positive domain on early endosomes but fail to continue into perinuclear recycling endosomes. We thus determined whether GFP-Rab11aS25N expression enhanced M_4 colocalization with Rab4. In cells expressing inactive Rab11aS25N, the morphology of Rab4-positive early endosomes was similar to pEGFP vector-transfected control cells. In pEGFP vector-transfected control cells, M_4 showed ~46 ± 2% (n = 16) colocalization with Rab4 (Fig. 5*B*). Expression of GFP-Rab11aS25N reduced M_4 colocalization with Rab4 (35 ± 2%; n = 16; $p <$

0.001). Therefore, expression of GFP-Rab11aS25N did not cause retention of M_4 in either EEA1- or Rab4-positive early endosomes.

GFP-Rab11aS25N expression may enhance trafficking of M_4 to a late endosomal–degradative pathway. Rab7 plays a role in trafficking from early sorting endosomes to late endosomes (Chavrier et al., 1990; Feng et al., 1995). Thus, if targeting of M_4 to late endosomes is enhanced by GFP-Rab11aS25N expression, M_4 colocalization with Rab7 should be enhanced. In vector-transfected cells (Fig. 5*C*), M_4 showed a perinuclear localization and Rab7 localized to small puncta throughout the cells. The morphology of Rab7-positive endosomes did not appear to be altered by expression of GFP-Rab11aS25N. Furthermore, colocalization of M_4 with Rab7 did not appear to be enhanced in GFP-Rab11sS25N-expressing cells. M_4 colocalization with Rab7 is 48 ± 2% ($n = 16$) in control cells and 49 ± 1% ($n = 16$; p = NS) in Rab11aS25N-expressing cells. Thus, expression of inactive GFP-Rab11aS25N does not enhance targeting of M_4 to a Rab7-positive late endosomal pathway.

M_4 recycling is Rab11a dependent

Because expression of dominant negative Rab11aS25N prevented trafficking of M_4 to perinuclear recycling endosomes, we determined whether inhibiting Rab11a activity also affected M_4 recovery to the cell surface. In contrast to control cells (Fig. 2), in GFP-Rab11aS25N-expressing cells, M_4 distribution remained dispersed throughout the cytosol and showed minimal return to the cell surface, followed by 60 min CCh washout (Fig. 6*A*).

To quantitate M_4 recycling, the percentage of M_4 that colocalized with the Na^+/K^+ ATPase was measured on confocal images. Because of low transfection efficiency in PC12 cells, measurements of the effects of mutant Rab11a expression would not normally be possible using traditional methods, such as binding assays or cell surface biotinylation. However, quantitative immunocytochemistry in single cells revealed that GFP-Rab11aS25N expression had a dramatic effect on M_4 recycling. Expression of GFP-Rab11aS25N inhibited M_4 recycling after CCh stimulation and 60 min washout relative to vector-transfected control cells ($p < 0.001$) (Fig. 6*B*). However, the inhibition was not complete, and, by 180 min, M_4 eventually returned to the cell surface. Quantitative immunocytochemistry revealed that the extent of cell surface M_4 in GFP-Rab11aS25N-expressing cells was similar to vector-transfected control cells 180 min after CCh washout (p = NS). The inhibition of M_4 recycling was specific for inhibition of Rab11a activity and not a result of general overexpression of Rab proteins because expression of dominant negative Rab5a does not affect the extent M_4 recycling (data not shown). These findings indicate that Rab11a GTPase activity plays an important role in the normal recovery of M_4 to the cell surface.

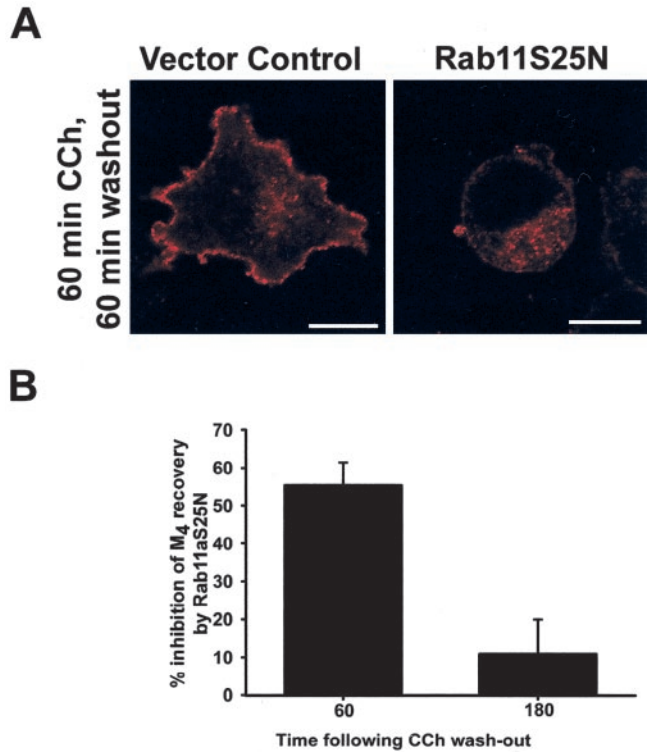

Figure 6. Constitutively GDP-bound Rab11aS25N impairs M_4 recycling. Cells were treated with CCh for 60 min, rinsed, and incubated in media alone for 60 or 180 min. *A*, After CCh treatment and washout, in cells expressing Rab11aS25N, M_4 showed little recovery to the cell surface compared with vector-transfected control cells and localized to small, intracellular puncta. Scale bars, 10 μm. *B*, The amount of M_4 recovery to the cell surface was measured by quantitation of confocal images, and the percentage of inhibition of M_4 recycling by Rab11aS25N was calculated relative to vector-transfected control cells. M_4 recycling was dramatically inhibited by Rab11aS25N expression 60 min after agonist washout. However, M_4 eventually returned to the cell surface 3 hr after agonist washout such that the percentage of inhibition of M_4 recycling was minimal after this prolonged time point.

The myosin Vb tail enhances concentration of M_4 in perinuclear endosomes

Recent studies have demonstrated that the active GTP-bound form of Rab11a can interact with the C-terminal tail domain of myosin Vb, and overexpression of a myosin Vb tail construct lacking its motor domain inhibits recycling of TfnR out of the perinuclear compartment in HeLa cells (Lapierre et al., 2001). Therefore, because M_4 recycling requires Rab11a activity, we determined whether myosin Vb also plays a role in M_4 return to the cell surface. PC12 cells were transfected with a GFP-myosin Vb tail construct that contains the Rab11a binding domain but lacks the myosin Vb motor domain. Consistent with previous findings (Lapierre et al., 2001), GFP-myosin Vb tail showed a concentrated localization near the nucleus (Fig. 7*A*). At baseline, the expression of the myosin Vb tail enhanced M_4 intracellular localization. To quantitate the effect of myosin Vb tail expression on the proportion of intracellular M_4, the percentage of cell surface M_4 that colocalized with the Na^+/K^+ ATPase was measured. In untreated cells, M_4 showed a small but statistically significant 11% decrease in colocalization with the Na^+/K^+ ATPase in cells expressing the myosin Vb tail compared with vector-transfected control cells ($p < 0.01$). These results are consistent with previous findings that M_4 shows a small amount of atropine-sensitive endocytic activity at baseline resulting from basal release of ACh (Volpicelli et al., 2001).

After 60 min CCh treatment, M_4 showed enhanced concentration in perinuclear endosomes in cells expressing the myosin Vb tail relative to control cells (Fig. 1), and M_4 showed extensive colocalization with the GFP-myosin Vb tail (Fig. 7*B*). Expression of the myosin Vb tail also significantly enhanced M_4 colocalization with the TfnR relative to vector-transfected control cells. M_4 colocalization with the TfnR in vector-transfected control cells was 51 ± 3% compared with 71 ± 3% ($p < 0.001$) in myosin Vb tail-expressing cells. Thus, the dominant negative myosin Vb tail enhances M_4 accumulation in perinuclear recycling endosomes.

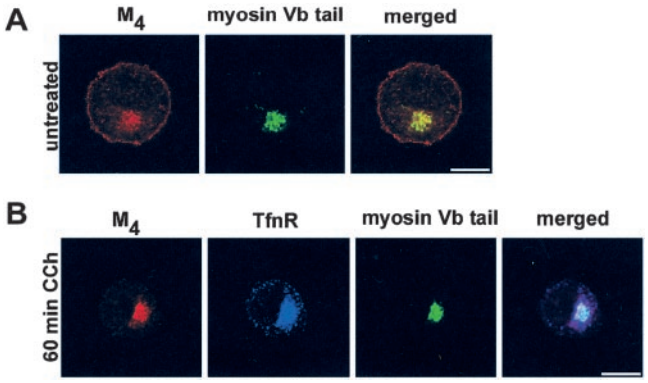

Figure 7. The myosin Vb tail enhances M_4 accumulation in perinuclear endosomes. *A*, Myosin Vb tail-GFP showed a concentrated, perinuclear localization. In untreated cells expressing the myosin Vb tail, M_4 (*red*) localized to the cell surface but also showed some accumulation intracellularly. Scale bar, 10 μm. *B*, Expression of the myosin Vb tail enhanced M_4 concentration in the perinuclear compartment after 60 min CCh treatment. The TfnR (*blue*) also showed enhanced accumulation in the perinuclear compartment, and M_4, the TfnR, and the myosin Vb tail (*green*) colocalized extensively (visualized as *white* in the merged image). Scale bar, 10 μm.

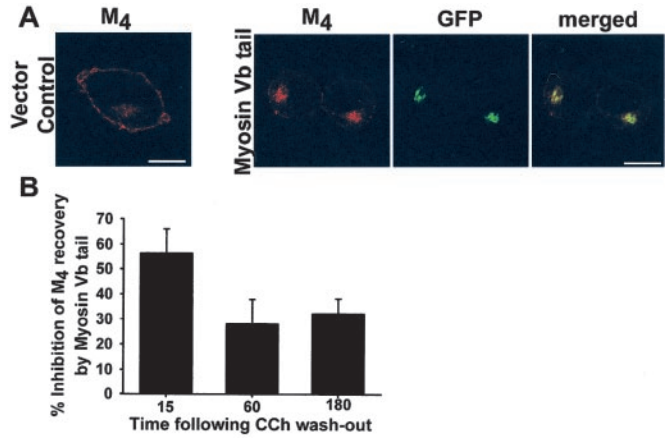

Figure 8. The myosin Vb tail prevents M_4 recycling. *A*, Cells were treated with CCh for 60 min, rinsed, and incubated in media alone for 60 min. As expected, in vector-transfected control cells, M_4 returned to the cell surface. In cells expressing the myosin Vb tail, the majority of M_4 remained in perinuclear recycling endosomes, although a small amount of M_4 returned to the cell surface. Scale bars, 10 μm. *B*, The amount of M_4 recovery to the cell surface was measured by quantitation of confocal images, and the percentage of inhibition of M_4 recycling by the myosin Vb tail was calculated relative to vector-transfected control cells. Expression of the myosin Vb tail dramatically inhibited M_4 recycling 15 min after CCh washout. M_4 recycling remained impaired by the myosin Vb tail for 60 min and as long as 180 min after CCh washout.

The myosin Vb tail inhibits M_4 recycling

Previous studies have suggested that expression of the myosin Vb tail inhibits transit of recycling cargo out from the perinuclear compartment back to the cell surface (Lapierre et al., 2001). We therefore determined the effects of GFP-myosin Vb tail expression on recycling. As expected, M_4 returned to the cell surface after 60 min CCh treatment and 60 min washout in vector-transfected control cells. However, in GFP-myosin Vb tail-expressing cells, the majority of M_4 was retained in the perinuclear compartment with little recovery by 60 min washout (Fig. 8*A*). The dramatic ability of dominant negative myosin Vb tail to inhibit M_4 recycling was apparent as early as 15 min after CCh washout and remained for up to 3 hr (Fig. 8*B*). Quantitation of the percentage of M_4 recycling after agonist treatment and washout showed that GFP-myosin Vb tail expression significantly inhibited M_4 recycling relative to vector-transfected control cells at 15, 60, and 180 min after CCh washout ($p < 0.001$). Therefore, the myosin Vb tail concentrated M_4 in perinuclear endosomes and functionally impeded M_4 trafficking back to the cell surface, indicating that myosin Vb plays a key role in M_4 recycling.

DISCUSSION

After agonist stimulation and internalization, the dynamic regulation of GPCR responsiveness after agonist stimulation is determined by a balance between degradation and recycling. Although the molecular mechanisms regulating GPCR internalization have received extensive study, the molecules involved in targeting GPCRs to the recycling pathway have only received attention recently. We show that, during prolonged agonist stimulation, M_4 accumulates in perinuclear endosomes, in which it colocalizes with TfnR and Rab11a. Expression of mutant forms of Rab11a and myosin Vb dramatically impair M_4 recycling. Thus, the results presented here indicate that M_4 receptors traffic through a specific recycling pathway through mechanisms dependent on both Rab11a and myosin Vb.

Previously, we demonstrated that, initially after agonist-induced internalization, M_4 traffics to peripherally distributed Rab5a-positive early endosomes (Volpicelli et al., 2001). We now extend these findings by showing that, with prolonged stimulation, M_4 traffics from early endosomes to perinuclear recycling endosomes, in which it colocalizes with the TfnR and Rab11a, markers for the perinuclear recycling compartment (Hopkins and Trowbridge, 1983; Yamashiro et al., 1984; Hopkins et al., 1990, 1994; Ghosh et al., 1994; Ullrich et al., 1996; Green et al., 1997; Ren et al., 1998; Casanova et al., 1999; Sonnichsen et al., 2000; Wang et al., 2001). Rab11a activity is required for M_4 recycling because expression of the constitutively GDP-bound form of Rab11a, Rab11aS25N, alters M_4 trafficking through the recycling pathway and severely impairs M_4 recycling after CCh washout. Other GPCRs localize to perinuclear endosomes after internalization (von Zastrow and Kobilka, 1992; Tolbert and Lameh, 1996), and some subtypes have been shown to colocalize with Rab11a (Moore et al., 1999; Innamorati et al., 2001; Kreuzer et al., 2001; Hunyady et al., 2002). Our study is the first to demonstrate that recycling of the M_4 subtype of GPCR requires Rab11a activity and indicates that the perinuclear endosomal compartment may be a common recycling pathway for multiple GPCR subtypes.

After internalization to early endosomes, receptors targeted for recycling traffic to perinuclear recycling endosomes (Mellman, 1996). In cells expressing Rab11aS25N, M_4 does not accumulate in perinuclear endosomes but localizes to small puncta with a vesicular appearance dispersed throughout the cell. Studies in nonpolarized cells suggest that Rab11aS25N impairs recycling by preventing receptor traffic from early endosomes (Ullrich et al., 1996; Ren et al., 1998). Thus, M_4 should accumulate in early endosomes in cells expressing Rab11aS25N, within either an EEA1-positive domain or a Rab4 domain. However, our results demonstrate that internalized M_4 does not show enhanced colocalization with EEA1 or Rab4 in Rab11aS25N-expressing cells. Therefore, unlike the TfnR, in this cell system, inactivation of Rab11a does not appear to prevent M_4 transit from early endosomes. Expression of Rab11aS5N also does not enhance M_4

colocalization with Rab7 and therefore Rab11aS5N does not enhance M_4 trafficking to a late endosomal–degradative pathway. Furthermore, because the cells were treated with the protein synthesis inhibitor cycloheximide, M_4 localization to biosynthetic compartments is minimal. However, M_4 does show colocalization with the TfnR in Rab11aS25N-expressing cells, identifying this compartment as an early endosomal compartment. These data thus suggest that M_4 traffics from early endosomes to recycling endosomes via an intermediate vesicular–early endosomal compartment and that active Rab11a is required for trafficking of these intermediate vesicles to perinuclear recycling endosomes. An alternative explanation is that, in cells expressing Rab11aS25N, M_4 traffics to recycling endosomes, but accumulation of tubules–vesicles near the nucleus is prevented. Inhibition of Rab11a activity could also alter recycling system morphology by blocking association of vesicles with Rab11a effectors, (Prekeris et al., 2000, 2001; Hales et al., 2001), including interaction with the myosin Vb motor protein (Lapierre et al., 2001).

Myosin Vb is an effector molecule that selectively interacts with the active GTP-bound Rab11a but not Rab11aS25N (Lapierre et al., 2001). Myosin Vb contains a tail domain that binds Rab11a, a neck domain containing calmodulin binding motifs and a motor head domain. Expression of the myosin Vb tail causes inhibition of TfnR recycling in HeLa cells, as well as basolateral to apical transcytosis and apical recycling in polarized Madin-Darby canine kidney cells (Lapierre et al., 2001). In this study, expression of the myosin Vb tail enhances accumulation of M_4 in the perinuclear compartment and inhibits recycling, even at prolonged time points after agonist washout. Thus, in myosin Vb tail-expressing cells, Rab11a-positive vesicles containing M_4 can accumulate in the perinuclear compartment, but they cannot exit because myosin Vb cannot mobilize vesicles out of perinuclear compartment back to cell surface. Integrity of the actin cytoskeleton is necessary for targeting GPCRs to the recycling pathway. For example, disrupting the actin cytoskeleton targets the β-adrenergic receptor to the degradative pathway (Cao et al., 1999). Although we did not address the fate of M_4 in myosin Vb tail-expressing cells because of low transfection efficiency in PC12 cells, it is possible that preventing myosin Vb interaction with the actin cytoskeleton would prevent sorting of M_4 to recycling pathway and enhance M_4 degradation. Regardless of the mechanism by which myosin Vb directs M_4 trafficking back to the cell surface, we show for the first time that a specific motor protein is involved in GPCR recycling.

In summary, after agonist stimulation, M_4 internalizes from the cell surface sequentially to Rab5a-positive early endosomes (Volpicelli et al., 2001) and then through a recycling endosomal system containing Rab11a and myosin Vb. Active Rab11a and myosin Vb are required for recycling of vesicles containing M_4 back to the cell surface, likely mediated in part via an interaction between myosin Vb and the actin cytoskeleton. M_4 plays an important role in locomotor activity (Gomeza et al., 1999), as the primary cholinergic autoreceptor in the striatum (Zhang et al., 2002) and as a target for the treatment of Alzheimer's disease (Bodick et al., 1997). Rab11a and myosin Vb are expressed in the brain (Sheehan et al., 1996; Zhao et al., 1996), and, thus, identifying that Rab11a and myosin Vb play key roles in M_4 recycling helps to understand the mechanisms by which neurons may maintain responsiveness to ACh stimulation. Overall, these studies indicate that specific trafficking pathways serve to direct the accurate recycling of particular GPCRs to the plasma membrane.

REFERENCES

Anborgh PH, Seachrist JL, Dale LB, Ferguson SS (2000) Receptor/beta-arrestin complex formation and the differential trafficking and resensitization of beta2-adrenergic and angiotensin II type 1A receptors. Mol Endocrinol 14:2040–2053.

Berkeley JL, Levey AI (2000) Muscarinic activation of mitogen-activated protein kinase in PC12 cells. J Neurochem 75:487–493.

Bernard V, Levey AI, Bloch B (1999) Regulation of the subcellular distribution of m4 muscarinic acetylcholine receptors in striatal neurons *in vivo* by the cholinergic environment: evidence for regulation of cell surface receptors by endogenous and exogenous stimulation. J Neurosci 19:10237–10249.

Bloch B, Dumartin B, Bernard V (1999) In vivo regulation of intraneuronal trafficking of G protein-coupled receptors for neurotransmitters. Trends Pharmacol Sci 20:315–319.

Bodick NC, Offen WW, Levey AI, Cutler NR, Gauthier SG, Satlin A, Shannon HE, Tollefson GD, Rasmussen K, Bymaster FP, Hurley DJ, Potter WZ, Paul SM (1997) Effects of xanomeline, a selective muscarinic receptor agonist, on cognitive function and behavioral symptoms in Alzheimer disease. Arch Neurol 54:465–473.

Bogatkewitsch GS, Lenz W, Jakobs KH, Van Koppen CJ (1996) Receptor internalization delays m4 muscarinic acetylcholine receptor resensitization at the plasma membrane. Mol Pharmacol 50:424–429.

Cao TT, Deacon HW, Reczek D, Bretscher A, von Zastrow M (1999) A kinase-regulated PDZ-domain interaction controls endocytic sorting of the beta2-adrenergic receptor. Nature 401:286–290.

Carroll RC, Beattie EC, von Zastrow M, Malenka RC (2001) Role of AMPA receptor endocytosis in synaptic plasticity. Nat Rev Neurosci 2:315–324.

Casanova JE, Wang X, Kumar R, Bhartur SG, Navarre J, Woodrum JE, Altschuler Y, Ray GS, Goldenring JR (1999) Association of Rab25 and Rab11a with the apical recycling system of polarized Madin-Darby canine kidney cells. Mol Biol Cell 10:47–61.

Chavrier P, Parton RG, Hauri HP, Simons K, Zerial M (1990) Localization of low molecular weight GTP binding proteins to exocytic and endocytic compartments. Cell 62:317–329.

Felder CC, Porter AC, Skillman TL, Zhang L, Bymaster FP, Nathanson NM, Hamilton SE, Gomeza J, Wess J, McKinzie DL (2001) Elucidating the role of muscarinic receptors in psychosis. Life Sci 68:2605–2613.

Feng Y, Press B, Wandinger-Ness A (1995) Rab 7: an important regulator of late endocytic membrane traffic. J Cell Biol 131:1435–1452.

Finn AK, Whistler JL (2001) Endocytosis of the mu opioid receptor reduces tolerance and a cellular hallmark of opiate withdrawal. Neuron 32:829–839.

Ghosh RN, Gelman DL, Maxfield FR (1994) Quantification of low density lipoprotein and transferrin endocytic sorting HEp2 cells using confocal microscopy. J Cell Sci 107:2177–2189.

Gomeza J, Zhang L, Kostenis E, Felder C, Bymaster F, Brodkin J, Shannon H, Xia B, Deng C, Wess J (1999) Enhancement of D1 dopamine receptor-mediated locomotor stimulation in M(4) muscarinic acetylcholine receptor knockout mice. Proc Natl Acad Sci USA 96:10483–10488.

Green EG, Ramm E, Riley NM, Spiro DJ, Goldenring JR, Wessling-Resnick M (1997) Rab11 is associated with transferrin-containing recycling compartments in K562 cells. Biochem Biophys Res Commun 239:612–616.

Hales CM, Griner R, Hobdy-Henderson KC, Dorn MC, Hardy D, Kumar R, Navarre J, Chan EK, Lapierre LA, Goldenring JR (2001) Identification and characterization of a family of Rab11-interacting proteins. J Biol Chem 276:39067–39075.

He L, Fong J, von Zastrow M, Whistler JL (2002) Regulation of opioid receptor trafficking and morphine tolerance by receptor oligomerization. Cell 108:271–282.

Hersch SM, Gutekunst CA, Rees HD, Heilman CJ, Levey AI (1994) Distribution of M_1–M_4 muscarinic receptor proteins in the rat striatum: light and electron microscopic immunocytochemistry using subtype-specific antibodies. J Neurosci 14:3351–3363.

Hopkins CR, Trowbridge IS (1983) Internalization and processing of transferrin and the transferrin receptor in human carcinoma A431 cells. J Cell Biol 97:508–521.

Hopkins CR, Gibson A, Shipman M, Miller K (1990) Movement of internalized ligand-receptor complexes along a continuous endosomal reticulum. Nature 346:335–339.

Hopkins CR, Gibson A, Shipman M, Strickland DK, Trowbridge IS (1994) In migrating fibroblasts, recycling receptors are concentrated in narrow tubules in the pericentriolar area, and then routed to the plasma membrane of the leading lamella. J Cell Biol 125:1265–1274.

Hunyady L, Baukal AJ, Gaborik Z, Olivares-Reyes JA, Bor M, Szaszak M, Lodge R, Catt KJ, Balla T (2002) Differential PI 3-kinase dependence of early and late phases of recycling of the internalized AT1 angiotensin receptor. J Cell Biol 157:1211–1222.

Innamorati G, Le Gouill C, Balamotis M, Birnbaumer M (2001) The long and the short cycle. Alternative intracellular routes for trafficking of G-protein-coupled receptors. J Biol Chem 276:13096–13103.

Koenig JA, Edwardson JM (1997) Endocytosis and recycling of G protein-coupled receptors. Trends Pharmacol Sci 18:276–287.
Kreuzer OJ, Krisch B, Dery O, Bunnett NW, Meyerhof W (2001) Agonist-mediated endocytosis of rat somatostatin receptor subtype 3 involves beta-arrestin and clathrin coated vesicles. J Neuroendocrinol 13:279–287.
Krudewig R, Langer B, Vogler O, Markschies N, Erl M, Jakobs KH, van Koppen CJ (2000) Distinct internalization of M2 muscarinic acetylcholine receptors confers selective and long-lasting desensitization of signaling to phospholipase C. J Neurochem 74:1721–1730.
Lapierre LA, Kumar R, Hales CM, Navarre J, Bhartur SG, Burnette JO, Provance Jr DW, Mercer JA, Bahler M, Goldenring JR (2001) Myosin vb is associated with plasma membrane recycling systems. Mol Biol Cell 12:1843–1857.
Lefkowitz RJ (1998) G protein-coupled receptors. III. New roles for receptor kinases and beta-arrestins in receptor signaling and desensitization. J Biol Chem 273:18677–18680.
Levey AI, Kitt CA, Simonds WF, Price DL, Brann MR (1991) Identification and localization of muscarinic acetylcholine receptor proteins in brain with subtype-specific antibodies. J Neurosci 11:3218–3226.
Mellman I (1996) Endocytosis and molecular sorting. Annu Rev Cell Dev Biol 12:575–625.
Moore RH, Tuffaha A, Millman EE, Dai W, Hall HS, Dickey BF, Knoll BJ (1999) Agonist-induced sorting of human beta2-adrenergic receptors to lysosomes during downregulation. J Cell Sci 112:329–338.
Muriel MP, Bernard V, Levey AI, Laribi O, Abrous DN, Agid Y, Bloch B, Hirsch EC (1999) Levodopa induces a cytoplasmic localization of D1 dopamine receptors in striatal neurons in Parkinson's disease. Ann Neurol 46:103–111.
Prekeris R, Klumperman J, Scheller RH (2000) A Rab11/Rip11 protein complex regulates apical membrane trafficking via recycling endosomes. Mol Cell 6:1437–1448.
Prekeris R, Davies JM, Scheller RH (2001) Identification of a novel Rab11/25 binding domain present in Eferin and Rip proteins. J Biol Chem 276:38966–38970.
Ren M, Xu G, Zeng J, De Lemos-Chiarandini C, Adesnik M, Sabatini DD (1998) Hydrolysis of GTP on rab11 is required for the direct delivery of transferrin from the pericentriolar recycling compartment to the cell surface but not from sorting endosomes. Proc Natl Acad Sci USA 95:6187–6192.
Roche KW, Standley S, McCallum J, Dune Ly C, Ehlers MD, Wenthold RJ (2001) Molecular determinants of NMDA receptor internalization. Nat Neurosci 4:794–802.
Rubino M, Miaczynska M, Lippe R, Zerial M (2000) Selective membrane recruitment of EEA1 suggests a role in directional transport of clathrin-coated vesicles to early endosomes. J Biol Chem 275:3745–3748.
Seachrist JL, Anborgh PH, Ferguson SS (2000) beta 2-adrenergic receptor internalization, endosomal sorting, and plasma membrane recycling are regulated by rab GTPases. J Biol Chem 275:27221–27228.
Sheehan D, Ray GS, Calhoun BC, Goldenring JR (1996) A somatodendritic distribution of Rab11 in rabbit brain neurons. NeuroReport 7:1297–1300.
Sonnichsen B, De Renzis S, Nielsen E, Rietdorf J, Zerial M (2000) Distinct membrane domains on endosomes in the recycling pathway visualized by multicolor imaging of Rab4, Rab5, and Rab11. J Cell Biol 149:901–914.
St. John PA, Gordon H (2001) Agonists cause endocytosis of nicotinic acetylcholine receptors on cultured myotubes. J Neurobiol 49:212–223.
Szekeres PG, Koenig JA, Edwardson JM (1998) Involvement of receptor cycling and receptor reserve in resensitization of muscarinic responses in SH-SY5Y human neuroblastoma cells. J Neurochem 70:1694–1703.
Tolbert LM, Lameh J (1996) Human muscarinic cholinergic receptor Hm1 internalizes via clathrin-coated vesicles. J Biol Chem 271:17335–17342.
Trejo J, Coughlin SR (1999) The cytoplasmic tails of protease-activated receptor-1 and substance P receptor specify sorting to lysosomes versus recycling. J Biol Chem 274:2216–2224.
Tsao PI, von Zastrow M (2000) Type-specific sorting of G protein-coupled receptors after endocytosis. J Biol Chem 275:11130–11140.
Ullrich O, Horiuchi H, Bucci C, Zerial M (1994) Membrane association of Rab5 mediated by GDP-dissociation inhibitor and accompanied by GDP/GTP exchange. Nature 368:157–160.
Ullrich O, Reinsch S, Urbe S, Zerial M, Parton RG (1996) Rab11 regulates recycling through the pericentriolar recycling endosome. J Cell Biol 135:913–924.
van der Sluijs P, Hull M, Webster P, Male P, Goud B, Mellman I (1992) The small GTP-binding protein rab4 controls an early sorting event on the endocytic pathway. Cell 70:729–740.
Volpicelli LA, Lah JJ, Levey AI (2001) Rab5-dependent trafficking of the m4 muscarinic acetylcholine receptor to the plasma membrane, early endosomes, and multivesicular bodies. J Biol Chem 276:47590–47598.
von Zastrow M, Kobilka BK (1992) Ligand-regulated internalization and recycling of human beta 2-adrenergic receptors between the plasma membrane and endosomes containing transferrin receptors. J Biol Chem 267:3530–3538.
Wang H, Han H, Zhang L, Shi H, Schram G, Nattel S, Wang Z (2001) Expression of multiple subtypes of muscarinic receptors and cellular distribution in the human heart. Mol Pharmacol 59:1029–1036.
Whistler JL, Chuang HH, Chu P, Jan LY, von Zastrow M (1999) Functional dissociation of mu opioid receptor signaling and endocytosis: implications for the biology of opiate tolerance and addiction. Neuron 23:737–746.
Yamashiro DJ, Tycko B, Fluss SR, Maxfield FR (1984) Segregation of transferrin to a mildly acidic (pH 6.5) para-Golgi compartment in the recycling pathway. Cell 37:789–800.
Zhang W, Basile AS, Gomeza J, Volpicelli LA, Levey AI, Wess J (2002) Characterization of central inhibitory muscarinic autoreceptors by the use of muscarinic acetylcholine receptor knock-out mice. J Neurosci 22:1709–1717.
Zhao LP, Koslovsky JS, Reinhard J, Bahler M, Witt AE, Provance Jr DW, Mercer JA (1996) Cloning and characterization of myr 6, an unconventional myosin of the dilute/myosin-V family. Proc Natl Acad Sci USA 93:10826–10831.